



Published in final edited form as:

Vascul Pharmacol. 2015 ; 0: 59–66. doi:10.1016/j.vph.2015.03.015.

Sparstolonin B suppresses rat vascular smooth muscle cell proliferation, migration, inflammatory response and lipid accumulation

Qing Liu^{1,2}, Jianping Li¹, Qiaoli Liang³, Dawei Wang², Yi Luo², Fang Yu⁴, Joseph S. Janicki¹, and Daping Fan^{1,*}

¹Department of Cell Biology and Anatomy, University of South Carolina School of Medicine, Columbia, SC 29209

²Guangdong Provincial Hospital of Chinese Medicine, The Second Clinical School of Medicine, Guangzhou University of Chinese Medicine, Guangzhou, 510405, China

³School of Pharmacy, Nanjing University of Chinese Medicine, Nanjing 210023, China

⁴Department of Nutrition and Food Hygiene, Fourth Military Medical University, Xi'an, 710032, China

Abstract

Vascular smooth muscle cells (VSMCs) play a crucial role in atherosclerotic lesion formation. Sparstolonin B (SsnB) is a TLR2/TLR4 antagonist that inhibits inflammatory responses in multiple cell types. Herein, we investigated if SsnB inhibited VSMC proliferation, migration, inflammatory response and lipid accumulation. We found that SsnB suppressed VSMC proliferation and migration induced by PDGF. SsnB significantly suppressed the expression of MCP-1, TNF α and IL-6 in VSMCs stimulated by either lipopolysaccharide (LPS) or PDGF. Erk1/2 and Akt signaling pathways, which are responsible for the VSMC inflammatory response, were activated by LPS or PDGF stimulation, and SsnB significantly inhibited their activation. SsnB also substantially suppressed the intracellular cholesterol accumulation in VSMCs loaded with acetylated LDL. Mechanistically, SsnB remarkably repressed LPS-induced up-regulation of CD36, which is responsible for lipid uptake, and dramatically reversed LPS-induced inhibition of ABCA1, which promotes the efflux of intracellular free cholesterol. In conclusion, our results indicate that SsnB significantly inhibits VSMC proliferation, migration, inflammatory responses and lipid accumulation. Along with the previously reported anti-inflammatory activities of SsnB on macrophages and vascular endothelial cells, our data strongly suggest that SsnB may be developed as a new anti-atherogenic therapy.

© 2015 Published by Elsevier Inc.

*Correspondence to Daping Fan, Department of Cell Biology and Anatomy, University of South Carolina School of Medicine, 6439 Garners Ferry Road, Columbia, SC 29209. Phone: 803-216-3806; Fax: 803-216-3846; daping.fan@uscmed.sc.edu.

Disclosures

None declared.

Publisher's Disclaimer: This is a PDF file of an unedited manuscript that has been accepted for publication. As a service to our customers we are providing this early version of the manuscript. The manuscript will undergo copyediting, typesetting, and review of the resulting proof before it is published in its final citable form. Please note that during the production process errors may be discovered which could affect the content, and all legal disclaimers that apply to the journal pertain.

Keywords

Sparstolonin B; VSMC; Atherogenesis; Inflammation; Lipid accumulation

1. Introduction

Atherosclerosis is the primary cause of heart attack and stroke and is the leading cause of death worldwide [1]. It is the result of both lipid deposition and chronic vascular inflammation [2–6]. While macrophages have been considered as the major driving force of atherogenesis, vascular smooth muscle cells (VSMCs) also significantly contribute to the process [7]. They play important roles in the progression of atherosclerotic plaques, during which VSMCs migrate into intima while acquiring an inflammatory and proliferative phenotype [8]. They engulf lipids and transform into foam cells, secrete inflammatory cytokines to contribute to the inflammatory scene in the lesion, and proliferate to promote the plaque volume growth [8]. Thus, targeting the pro-atherogenic phenotype of VSMCs may be developed as new anti-atherosclerotic therapies [9].

It is believed that TLRs, especially TLR4 and TLR2, play active roles in the acquisition of an inflamed and proliferative phenotype by VSMCs during atherogenesis [10]. Human VSMCs constitutively express TLR1, TLR3, TLR4 and TLR6 [11]; TLR2 expression can be induced by TLR3 and TLR4 stimuli in human coronary artery smooth muscle cells; whereas TLR2 is constitutively expressed in murine aortic smooth muscle cells as TLR4 [12]. Cultured VSMCs secrete IL-6 and MCP-1 in response to LPS or poly(I:C) stimulation; exposure of VSMCs to *C. pneumoniae* leads to TLR2-dependent MCP-1 release [11–14]. Cholesterol accumulation and inflammatory response reinforce each other in macrophages [15–18] and endothelial cells [19]; similarly, it is shown that under inflammatory stimulation, VSMCs acquire enhanced ability to take up native and modified LDL particles and transform into foam cells [20].

Sparstolonin B (SsnB), a compound isolated from the Chinese herb *Sparganium stoloniferum*, has been characterized by us previously as a selective TLR2 and TLR4 antagonist [21]. Our previous studies have shown that SsnB could attenuate inflammatory responses in macrophages [21] and endothelial cells [22], suggesting that SsnB may act as a potential therapeutic agent for inflammatory diseases, such as atherosclerosis. In addition to acting as a TLR2 and TLR4 antagonist, we also demonstrated that SsnB blocked cell cycle progression in human umbilical vein endothelial cell (HUVEC) and inhibited its pro-angiogenic functions. Moreover, SsnB potently attenuated cardiomyocyte inflammation in an ischemia and reperfusion injury model *in vitro* [23]. However, if and how SsnB affects VSMC function is unknown. In this study, we showed that SsnB significantly inhibited VSMC proliferation, migration, and inflammatory responses to LPS and PDGF, as well as lipid accumulation. Considering the critical role of VSMCs in atherosclerosis, and the anti-inflammatory activity of SsnB on macrophages and vascular endothelial cells, we expect that SsnB may be developed as a new agent for the prevention and treatment of atherosclerosis.

2. Materials and Methods

2.1 Cell culture

Vascular smooth muscle cells (VSMCs) used in this study were rat aortic smooth muscle cells. They were isolated from eight-week-old male Sprague-Dawley rats by enzymatic dispersion method [24]. Briefly, the rat thoracic aorta was isolated and cleaned of fat. The whole aorta was incubated with a digestion mixture containing collagenase I (1 mg/ml), elastase (0.5 mg/ml), and trypsin (1.25 mg/ml) (all from Sigma-Aldrich, St. Louis, MO) in serum-free Dulbecco's modified Eagle's medium (DMEM) (Invitrogen Life Technologies, Grand Island, NY) at 37°C for 10 min, then the adventitia including the endothelial cells was peeled off with forceps. The vessel was chopped into small blocks, rinsed and transferred to a sterile digestion mixture. Smooth muscle cells were released by further incubation for 4 h at 37°C. After centrifugation, the cells were resuspended and cultured in DMEM supplemented with 10% Fetal bovine serum (FBS), 100 U/mL penicillin, 100 µg/mL streptomycin, 8 mM HEPES, and 2 mM L-glutamine at 37 °C. The VSMCs were passaged at a ratio of 1:3 until confluence was reached. The morphology of VSMCs was observed under an inverted microscope, and their purity was confirmed by immunocytochemical localization of α-smooth-muscle actin. VSMCs were used from passages 4–8 in the following experiments.

2.2 SsnB treatment

SsnB was isolated from Chinese herb *S. stoloniferum*, and the purity was confirmed as described previously [21]. SsnB powder was dissolved in Dimethyl Sulfoxide (DMSO) as a stock solution of 50 mg/ml (186.6 mM). The stock solution was diluted with appropriate medium to desired concentration for cell treatment.

2.3 Cytotoxicity assay

LDH is normally retained in the cytosol until the sarcolemmal membrane is ruptured, after which it is free to diffuse into the surrounding media [25]. To determine the cytotoxicity of SsnB, both the culture medium and cell lysate were collected and the LDH activity was immediately detected at OD 490nm with a Spectra Max M5 Microplate Reader (Molecular Devices, Sunnyvale, CA) according to the manufacturer's instructions (Clontech, Mountain View, CA). Cell viability was calculated as the ratio of LDH amount in the cell lysate to the total LDH amount from both the medium and cell lysate.

2.4 Cell proliferation assays

Cell proliferation was measured by three methods: direct counting, LDH assay [26] and [³H] thymidine incorporation assay. Initially, VSMCs were seeded into 24-well cell culture plates at 3×10⁴/well and cultured in DMEM containing 10% FBS for 24 h. When the cells reached 70% confluence, the medium was replaced with serum-free DMEM (SFM). Cells were serum-starved for 12h before being stimulated by PDGF-BB (20 ng/ml; Sigma) in the absence or presence of SsnB at varied concentrations. For the direct cell counting, cells were trypsinized with Trypsin-EDTA and counted with a hemocytometer under microscope. For the LDH assay, cell lysate with 1% Triton-100 was collected and immediately assayed for

LDH activity as described above. For the [³H] thymidine incorporation assay, [³H] thymidine at 1 μCi/ml was added to the medium and the cells were incubated for 24 h. The cultures were then placed on ice and reactions were terminated by aspiration of the medium, followed by sequential washes with PBS containing 10% trichloroacetic acid. Acid-insoluble [³H] thymidine was lysed with 300 μl of 0.5N NaOH, and the lysate was mixed with 3 ml scintillation cocktail and quantified using a liquid scintillation counter (PerkinElmer, Waltham, MA).

2.5 Cell migration assays

Cell migration was determined by wound-healing assay and transwell migration assay. For the wound-healing assay, cells were seeded into 12-well plates at 8×10^4 cells/well and cultured in DMEM containing 10% FBS at 37 °C for 24 h. When the cells reached confluence, the medium was replaced with serum-free DMEM. The monolayer cells were serum-starved for 12 h before being wounded with a sterile cell scraper. After washing, the cells were stimulated by PDGF-BB (20 ng/ml) in the absence or presence SsnB at varied concentrations for 24 h. The migration distances between the leading edge of the migrating cells, and the migrated cell areas were measured and analyzed with the Image-Pro Plus 6.0 software (Media Cybernetics, Rockville, MD). For the transwell migration assay, cells were serum-starved for 12 h and 3×10^4 cells/well in 150 μl serum-free DMEM were seeded onto the upper inserts of the 24-well plates (8 μm pore size, Corning, New York). 500 μl of the serum-free DMEM with or without PDGF-BB in the absence or presence of SsnB was added to the lower chamber. Four hours later, cells remaining in the upper chamber were removed with a cotton swab, and the migrated cells situated on the lower side of membranes were fixed with 4% formaldehyde for 20 min, stained with 1 μg/ml DAPI for 1 min. For each sample, 10 random fields of the stained cells were photographed using an inverted wide-field fluorescence microscope (Eclipse E600, Nikon, Japan) at 100 x magnification. Cell numbers were counted using Image-Pro Plus 6.0.

2.6 quantitative real-Time PCR (qPCR)

Total RNA was extracted using TRIzol reagent (Life Technologies, Grand Island, NY) according to the manufacturers' instructions. Reverse transcription was performed using a First-strand cDNA Synthesis Kit (Bio-Rad, Hercules, CA). qPCR was carried out using iQ SYBR Green Supermix (Bio-Rad) on a CFX96 system (Bio-Rad). The primers (Integrated DNA Technologies, Coralville, IA) used in qPCR are listed as follows: rat 18s RNA (internal control) 5'-TGAGGCCATGATTAAGAGGG-3' (forward) and 5'-AGTCGGCATCGTTTATGGTC-3' (reverse); rat MCP-1, 5'-CCAATGAGTCGGCTGGAGAACT-3' (forward) and 5'-AGTGCTTGAGGTGGTTGTGGAA -3' (reverse); rat IL-6, 5'-AGGAGACTTCACAGAGGATACC-3' (forward) and 5'-TCCAGAAGACCAGAGCAGATT-3' (reverse); rat TNFα, 5'-TGGCGTGTTTCATCCGTTCTC-3' (forward) and 5'-ACTACTTCAGCGTCTCGTGTG-3' (reverse); rat CD36, 5'-TGTGAGTTGGCAAGAAGCAAGT-3' (forward) and 5'-GCACCAATAACGGCTCCAGTAA-3' (reverse); rat ABCA1, 5'-CTGACTGGAGATACCGCTGTGA-3' (forward) and 5'-CGCTTGTTACCGCCACTGTAG-3' (reverse). Samples were amplified using the following

program, 95°C for 10 min followed by 40 cycles of 95°C for 10 s, 58°C for 15 s, and 72°C for 20 s, then a melting curve analysis from 65°C to 95°C every 0.2°C. The abundance of each gene was calculated by relative quantification, with values for the target genes normalized with 18s RNA.

2.7 Western blot

Cells were lysed using the Lysis buffer (Cell signaling, Danvers, MA) on ice for 15 min, and the lysates were clarified by centrifugation at 4°C for 10 min at 13,000 rpm. After quantitation of protein concentration by Lowry assay, 30 µg (for Erk1/2) or 45 µg (for Akt and ABCA1) of total proteins were loaded onto 10% SDS-PAGE gels for electrophoresis at 100 V for 1.5 h. The proteins were then transferred to nitrocellulose membranes. The membranes were blocked for 1 h at room temperature with 5% non-fat dry milk, then incubated with primary antibodies against p-Erk1/2 and t-Erk1/2 (Millipore, Billerica, MA), p-Akt and t-Akt (Cell signaling), ABCA1 (Novus Biologicals, Littleton, CO) and β-actin (1:500~1:1000) overnight at 4°C. After washing with PBST, the membranes were incubated with HRP-conjugated secondary antibodies for 1 h at room temperature. Signal of target proteins was detected with an ECL kit (Pierce, Rockford, IL). The density of the bands in the images was quantified by Image-Pro Plus 6.0.

2.8 PI3K inhibition assay

PI3K activity ELISA assay was performed using a 96-well ELISA assay kit for detection of PI(3,4,5)P3 and purified PI3Kα (p100α/p85α) protein from Echelon Biosciences (Salt Lake City, UT) following the manufacturer's instructions. SsnB at various concentrations was added to the kinase reaction, and LY294002 was used as a positive control.

2.9 Oil Red O staining

To load VSMCs with lipid, cells were cultured with DMEM containing 1% FBS and 50 µg/ml acetylated LDL (ac-LDL) in the absence or presence of 10 ng/ml LPS for 24 h. Oil Red O staining was performed to evaluate the intracellular cholesterol level [27]. Briefly, after experimental treatment, the cells were rinsed by PBS and then fixed with 10% formalin for 30–60 min at room temperature. Formalin was discarded and 60% isopropanol was added into each well. Isopropanol was removed 5 min later and Oil Red O working solution was added. After another 5 min, Oil Red O was removed and Hematoxylin was added. Ten images in each sample were taken under a phase contrast microscope. Lipids appeared dark red and nuclei appeared blue.

2.10 Intracellular cholesterol quantification

The intracellular total and free cholesterol were measured by an Intracellular Cholesterol Quantitation Kit (Sigma-aldrich) according to the manufacturer's instructions. Briefly, after experimental treatment for 24 h, 2×10^6 cells were trypsinized with Trypsin-EDTA followed by centrifugation. Then the cell pellets were resuspended in a mix of chloroform: isopropanol: IGEPAL CA-630 (7:11:0.1). The samples were centrifuged at 13,000 g for 10 min to remove insoluble material. Then the organic phase was transferred to new tubes and air dried at 50°C for 30 min to remove chloroform, followed by blowing the samples with

nitrogen to remove any residual organic solvent. Then the lipid was dissolved with 200 μ l Cholesterol Assay Buffer and 50 μ l of the Reaction Mix was added to each standard and sample well in a 96-well plate, and incubated for 60 min at 37°C in dark. The absorbance was measured with a Spectra Max M5 Microplate Reader (Molecular Devices) at OD 570 nm. Concentrations of cholesterol were calculated by dividing the amount of cholesterol by the sample volume.

2.11 Cholesterol loading and efflux assay

Ac-LDL loading and cholesterol efflux of VSMCs were measured using a method similar to that used for macrophage cholesterol efflux measurement [28]. Briefly, rat VSMCs were cultured in 24-well plates in DMEM containing 10% FBS till confluence and further cultured in DMEM containing 0.25% FBS overnight, followed by loading with 50 μ g/ml ac-LDL incorporated with 3 H-cholesterol with or without LPS (10 ng/ml) and SsnB (10 μ M) for 24 h. Then efflux medium (DMEM containing 20 μ g/ml apoAI) was added to initiate cholesterol efflux for 24 h. 3 H radioactivity in efflux medium and cells were counted using a Beckman LS6500 liquid scintillation counter (Beckman Coulter, Indianapolis, IN). Cellular protein was determined using Lowry assay. Total cholesterol loading and cholesterol efflux efficiency were calculated.

2.11 Statistical Analysis

One-way analysis of variance (One-way ANOVA) was used for multiple group comparisons. If the data followed a Gaussian distribution, then Bonferroni's multiple comparisons were used as a post-test. Otherwise, the non-parametric KruskalWallis test and Dann's multiple comparison post-test were used to analyze the data. Student's *t* test was performed for two group comparisons. $p < 0.05$ was considered statistically significant. GraphPad Prism 5 software (GraphPad Software, San Diego, CA) was used for all of the statistical analysis.

3. Results

3.1 SsnB suppresses PDGF-induced VSMC proliferation

The cytotoxicity of SsnB on VSMC was evaluated by LDH assay. SsnB did not decrease VSMC viability until its concentration reached 100 μ M (Fig. 1A). Therefore, in all of the following experiments, the concentrations of SsnB were limited to 3, 10 or 30 μ M. Platelet-derived growth factor (PDGF) is a major factor that drives smooth muscle cell migration and proliferation in atherosclerosis [7, 29]. To test if SsnB inhibits PDGF-stimulated VSMC proliferation, direct cell counting, LDH assay and [3 H] thymidine incorporation assays were performed. Direct cell counting showed that PDGF treatment induced a 2-fold increase of VSMC proliferation. However, SsnB significantly inhibited VSMC proliferation in a dose-dependent manner (Fig 1B, C). LDH assay and [3 H] thymidine incorporation assay revealed similar inhibitory effects of SsnB on VSMC proliferation (Fig 1D, E).

3.2 SsnB inhibits PDGF-induced VSMC migration

Migration of VSMCs into the intima is a key early event in the pathogenesis of atherosclerosis [7, 30]. Thus, we tested the effects of SsnB on PDGF-stimulated VSMC

migration by the wound-healing and transwell assays. The wound healing assay results showed PDGF stimulation dramatically increased VSMC migration and thus reduced the wound width by 3-fold and increased the migration area by 2.5-fold, relative to untreated group (Fig 2A, B); while SsnB effectively inhibited PDGF-induced cell migration in a dose-dependent manner (Fig 2A–C). Transwell migration assay showed that PDGF promoted the migration of VSMC by 6-fold compared to the untreated group; and SsnB significantly inhibited PDGF-induced VSMC migration dose-dependently (Fig 2D, E).

3.3 SsnB suppresses LPS or PDGF-induced expression of inflammatory mediators in VSMCs

To examine if SsnB inhibits the inflammatory responses of VSMCs, we stimulated the cells with LPS or PDGF for 6 h in serum-free medium. MCP-1, TNF α and IL-6 levels were determined by quantitative real-time PCR. Fig 3A showed that MCP-1 mRNA level was significantly increased by 580- and 100-fold upon LPS and PDGF stimulation, respectively, relative to untreated group; while SsnB at 10 μ M reduced its levels by 3- and 45-fold compared to LPS and PDGF treated cells, respectively. Similarly, SsnB dramatically inhibited LPS and PDGF enhanced expression of TNF α and IL-6 (Fig 3B, C)

3.4 SsnB suppresses multiple signaling pathways in VSMCs

The Erk1/2 and PI3K/Akt signaling pathways are among the most important mechanisms responsible for VSMC proliferation, migration and inflammatory response [31–35]. Above data showed that SsnB suppressed PDGF-induced VSMC proliferation and migration. Thus, we determined if PDGF activated Erk1/2 and Akt pathways in VSMCs and if SsnB inhibited their activation. We found that phosphorylated Erk1/2 and Akt (p-Erk1/2 and p-Akt, respectively) levels were remarkably enhanced upon PDGF stimulation for 6 h, while their levels were gradually inhibited by increasing doses of SsnB (Fig 4A). However, total Erk1/2 (t-Erk1/2) and Akt (t-Akt) protein levels were not influenced by PDGF or SsnB (Fig 4A). We also noticed that SsnB inhibited the baseline p-Erk1/2 and p-Akt levels without PDGF treatment (Fig 4A). Similarly, LPS treatment induced a dramatic increase in phosphorylation of Erk1/2 and SsnB inhibited it dose-dependently (Fig 4B). While the mechanism by which SsnB suppresses PDGF signaling is unclear, we examined if SsnB directly inhibits PI3K activity by performing a PI3K activity ELISA assay. The result showed that SsnB suppressed PI3K p100 α activity with an IC₅₀ at ~14 μ M; while LY294002, a known PI3K inhibitor, displayed a more potent p100 α inhibitory activity with an IC₅₀ at 0.45 μ M (Fig 4C), similar to the previously reported data [36]. These results indicate that SsnB may inhibit PDGF and LPS induced cell proliferation, migration and inflammatory responses through its ability to block the Erk1/2 and PI3K/Akt signaling pathways.

3.5 SsnB attenuates cholesterol accumulation in acetylated LDL-treated VSMCs

During atherogenesis, VSMCs that migrate into the intima can engulf both native and modified LDL particles and transform into lipid-laden foam cells. Under the influence of the inflammatory cytokines, the VSMC foam cell formation is accelerated. We next examined if SsnB can diminish cholesterol accumulation in VSMCs. We incubated VSMCs with acetylated LDL (ac-LDL) for 24 h, and detected the accumulation of intracellular lipid droplets by Oil Red O staining. Unlike macrophages, which take up ac-LDL rapidly,

VSMCs did not drastically accumulate lipid upon ac-LDL loading for 24 h; however, with simultaneous LPS treatment, VSMCs accumulated significant amount of lipids, while SsnB treatment completely inhibited it (Fig 5A). To further quantify the effects of SsnB on lipid accumulation in VSMCs, we measured the intracellular total cholesterol and free cholesterol level by the Intracellular Cholesterol Quantitation Kit after the cells were treated with ac-LDL with or without LPS or SsnB for 24 h (Fig 5B, C). The intracellular total cholesterol and free cholesterol levels were increased from 184 ± 10 to 218 ± 18 $\mu\text{g/ml}$ and 112 ± 29 to 184 ± 9 $\mu\text{g/ml}$ by ac-LDL loading, respectively. Their levels were further dramatically elevated to 328 ± 21 and 297 ± 6 $\mu\text{g/ml}$, respectively with the addition of LPS treatment. However, SsnB significantly decreased their levels to 200 ± 11 and 198 ± 8 $\mu\text{g/ml}$, respectively. To further examine the mechanisms underlying the LPS-enhanced cholesterol accumulation and the effects of SsnB against it, we performed a cholesterol loading and efflux experiment using ^3H -cholesterol-incorporated ac-LDL. The result showed that while LPS dramatically increased ac-LDL uptake by VSMCs, SsnB significantly blunted the effects (Fig 5D). On the other hand, while LPS significantly reduced apoAI-mediated cholesterol efflux from VSMCs, SsnB substantially restored it (Fig 5E). These results suggested that SsnB could not only reduce LPS-enhanced cholesterol uptake by VSMCs, but can also improve cholesterol exit from VSMCs.

Among many molecules that contribute to cholesterol accumulation in VSMCs during atherogenesis, CD36 accounts for substantial portion of the lipid uptake [37–39], while ABCA1 is crucial for efflux of free cholesterol [40, 41]. Thus, we examined the effects of SsnB on the expression of CD36 and ABCA1 in VSMCs. It was shown that ac-LDL plus LPS treatment induced a 2- to 3-fold increase of CD36 mRNA level, which was reversed by SsnB (Fig 6A). Contrastingly, ABCA1 mRNA level was down-regulated by treatment of ac-LDL with LPS, whereas its level was strikingly enhanced by SsnB (Fig 6B). The up-regulation of ABCA1 by SsnB in VSMCs was further confirmed by western blot (Fig 6C, D).

4. Discussion

Growing evidence suggest that toll-like receptor (TLR) pathways are involved in plaque initiation and progression of atherosclerosis [42–45]. As one of the most important components of vascular walls, VSMC migration, proliferation and foam cell transformation are key events in the formation of atherosclerotic lesions and TLRs-mediated signaling pathways play important roles in these events [46]. SsnB is a TLR2/4 antagonist [21]; in this study, we examined the potential effects of SsnB on VSMCs in the context of atherogenesis. Our study, for the first time, demonstrated that SsnB significantly inhibited VSMC proliferation, migration, inflammatory response and lipid accumulation. Since our previous studies have shown that SsnB could attenuate inflammatory responses in macrophages and endothelial cells, which are also involved in the formation of atherosclerosis, the present study further suggest that SsnB may serve as a novel therapeutic agent for the prevention of atherosclerosis and resultant cardiovascular diseases.

VSMCs are involved throughout the development of atherosclerotic lesions [46]. Their migration into intima and subsequent proliferation are early events in neointimal formation

and substantially contribute to the atheroma volume during the later stages [7]. PDGF is a potent mitogen, produced by VSMCs, endothelial cells, and platelets in the injured vascular wall, and stimulates VSMC proliferation and migration at sites of stress [7, 47, 48]. It has been shown that suppression of PDGF receptor activation can inhibit VSMC proliferation by deactivating its downstream signaling molecules [49]. Therefore, we selected PDGF as an activator for VSMCs *in vitro*. Our study showed that SsnB significantly suppressed PDGF-induced VSMC proliferation and migration in a dose-dependent manner. Since there is no evidence to indicate that TLR2 and TLR4 are involved in PDGF-induced VSMC proliferation and migration, we suspect that the inhibitory activity of SsnB is independent of TLR2/4 and instead involves the intracellular signaling pathways in PDGF-stimulated VSMCs. These include the PLC γ 1, Akt and Erk1/2 signaling pathways which are activated by PDGF and its receptor (PDGFR) in VSMCs and are responsible for the cell proliferation, migration and angiogenesis of VSMCs [50, 51]. We found that SsnB dramatically attenuated PDGF stimulated Erk1/2 and Akt activation dose-dependently; and *in vitro* biochemical assay further showed that SsnB directly suppressed PI3K p100 α kinase activity. Chronic inflammation has been recognized as a crucial component in the development of atherosclerotic plaques. Exposure to LPS is known to induce pro-inflammatory cytokine expression in human VSMCs, macrophages and endothelial cells. LPS stimulated cell signaling pathways, such as Erk1/2, Akt and NF- κ B, can be activated during pathogenesis of atherosclerosis [50, 51]. Our study showed that SsnB apparently inhibited LPS-induced Erk1/2 phosphorylation but had only minor effects on the Akt and NF- κ B signaling pathways. Our data suggest that SsnB may exert the anti-atherogenic effects on VSMCs via blocking Erk1/2 and PI3K/Akt signaling pathways.

Foam cells are a hallmark and an obligatory component of atherosclerotic plaques. Although the majority of foam cells are derived from macrophages, VSMCs also contribute to the foam cell pool. VSMCs in the plaques acquire a proliferative and inflammatory phenotype, along with significantly enhanced lipid accumulation [20, 30, 52]. Like in the case of macrophages, CD36 is one of the major lipid uptake receptors in VSMCs, while ABCA1 plays a critical role in free cholesterol efflux from VSMCs [53, 54]. Our data indicated that ac-LDL alone did not alter the expression of CD36 and ABCA1 and, thus, no dramatic cholesterol accumulation was observed. However, concomitant treatment with LPS significantly increased CD36 and decreased ABCA1 expression in VSMCs and consequently was accompanied by substantial cholesterol, especially free cholesterol, accumulation. Interestingly, SsnB completely suppressed LPS-induced CD36 expression in VSMCs and reversed the reduction in ABCA1 expression, therefore, reduced LPS-enhanced cholesterol loading and restored LPS-impaired cholesterol efflux, eliminating LPS-exaggerated cholesterol accumulation in VSMCs.

Taken together, our results demonstrated that SsnB suppressed VSMC proliferation, migration, inflammatory responses and the lipid accumulation. Combined with our previous findings that SsnB effectively inhibited inflammation in macrophages and vascular endothelial cells and exerted anti-inflammatory effects during hypoxia-reoxygenation induced cardiomyocyte injury, we speculate that SsnB has the potential to be used as a therapeutic agent for the prevention of cardiovascular atherosclerotic disease. Additional

studies are being performed to determine if SsnB attenuates atherosclerosis in mouse models.

Acknowledgments

This work was supported by grants from national Institute of Health R21AT006767, R01HL116626 and P01AT003961-8455 (to DF) and from the National Natural Science Foundation of China 81173515 (to QL).

References

1. Faxon DP, Creager MA, Smith SC Jr, Pasternak RC, et al. *Circulation*. 2004; 109:2595–2604. [PubMed: 15173041]
2. Hansson GK. Inflammation, atherosclerosis, and coronary artery disease. *N Engl J Med*. 2005; 352:1685–1695. [PubMed: 15843671]
3. Lusis AJ. Atherosclerosis. *Nature*. 2000; 407:233–241. [PubMed: 11001066]
4. Ross R. Atherosclerosis--an inflammatory disease. *N Engl J Med*. 1999; 340:115–126. [PubMed: 9887164]
5. Libby P. Inflammation in atherosclerosis. *Nature*. 2002; 420:868–874. [PubMed: 12490960]
6. Steinberg D. Hypercholesterolemia and inflammation in atherogenesis: two sides of the same coin. *Mol Nutr Food Res*. 2005; 49:995–998. [PubMed: 16270285]
7. Louis SF, Zahradka P. Vascular smooth muscle cell motility: From migration to invasion. *Experimental and clinical cardiology*. 2010; 15:e75–85. [PubMed: 21264073]
8. Doran AC, Meller N, McNamara CA. Role of smooth muscle cells in the initiation and early progression of atherosclerosis. *Arterioscler Thromb Vasc Biol*. 2008; 28:812–819. [PubMed: 18276911]
9. Rudijanto A. The role of vascular smooth muscle cells on the pathogenesis of atherosclerosis. *Acta medica Indonesiana*. 2007; 39:86–93. [PubMed: 17933075]
10. Yang X, Coriolan D, Murthy V, Schultz K, et al. Proinflammatory phenotype of vascular smooth muscle cells: role of efficient Toll-like receptor 4 signaling. *Am J Physiol Heart Circ Physiol*. 2005; 289:H1069–1076. [PubMed: 15863460]
11. Yang X, Murthy V, Schultz K, Tatro JB, et al. Toll-like receptor 3 signaling evokes a proinflammatory and proliferative phenotype in human vascular smooth muscle cells. *Am J Physiol Heart Circ Physiol*. 2006; 291:H2334–2343. [PubMed: 16782847]
12. Yang X, Coriolan D, Schultz K, Golenbock DT, Beasley D. Toll-like receptor 2 mediates persistent chemokine release by *Chlamydia pneumoniae*-infected vascular smooth muscle cells. *Arterioscler Thromb Vasc Biol*. 2005; 25:2308–2314. [PubMed: 16179594]
13. Hong TJ, Ban JE, Choi KH, Son YH, et al. TLR-4 agonistic lipopolysaccharide upregulates interleukin-8 at the transcriptional and post-translational level in vascular smooth muscle cells. *Vascul Pharmacol*. 2009; 50:34–39. [PubMed: 18824136]
14. Stoll LL, Denning GM, Weintraub NL. Potential role of endotoxin as a proinflammatory mediator of atherosclerosis. *Arterioscler Thromb Vasc Biol*. 2004; 24:2227–2236. [PubMed: 15472123]
15. Shibata N, Glass CK. Regulation of macrophage function in inflammation and atherosclerosis. *J Lipid Res*. 2009; 50(Suppl):S277–281. [PubMed: 18987388]
16. Castrillo A, Tontonoz P. Nuclear receptors in macrophage biology: at the crossroads of lipid metabolism and inflammation. *Annu Rev Cell Dev Biol*. 2004; 20:455–480. [PubMed: 15473848]
17. Joseph SB, Bradley MN, Castrillo A, Bruhn KW, et al. LXR-dependent gene expression is important for macrophage survival and the innate immune response. *Cell*. 2004; 119:299–309. [PubMed: 15479645]
18. Zhao Y, Pennings M, Hildebrand RB, Ye D, et al. Enhanced foam cell formation, atherosclerotic lesion development, and inflammation by combined deletion of ABCA1 and SR-BI in Bone marrow-derived cells in LDL receptor knockout mice on western-type diet. *Circ Res*. 107:e20–31. [PubMed: 21071707]

19. Mullick AE, Soldau K, Kiosses WB, Bell TA 3rd, et al. Increased endothelial expression of Toll-like receptor 2 at sites of disturbed blood flow exacerbates early atherogenic events. *J Exp Med*. 2008; 205:373–383. [PubMed: 18250194]
20. Lacolley P, Regnault V, Nicoletti A, Li Z, Michel JB. The vascular smooth muscle cell in arterial pathology: a cell that can take on multiple roles. *Cardiovascular research*. 2012; 95:194–204. [PubMed: 22467316]
21. Liang Q, Wu Q, Jiang J, Duan J, et al. Characterization of sparstolonin B, a Chinese herb-derived compound, as a selective Toll-like receptor antagonist with potent anti-inflammatory properties. *J Biol Chem*. 2011; 286:26470–26479. [PubMed: 21665946]
22. Liang Q, Yu F, Cui X, Duan J, et al. Sparstolonin B suppresses lipopolysaccharide-induced inflammation in human umbilical vein endothelial cells. *Archives of pharmacal research*. 2013; 36:890–896. [PubMed: 23604718]
23. Liu Q, Wang J, Liang Q, Wang D, et al. Sparstolonin B attenuates hypoxia-reoxygenation-induced cardiomyocyte inflammation. *Exp Biol Med (Maywood)*. 2014; 239:376–384. [PubMed: 24477822]
24. Jiang F, Guo N, Dusting GJ. Modulation of nicotinamide adenine dinucleotide phosphate oxidase expression and function by 3',4'-dihydroxyflavonol in phagocytic and vascular cells. *The Journal of pharmacology and experimental therapeutics*. 2008; 324:261–269. [PubMed: 17916758]
25. Wei H, L'Ecuyer T, Vander Heide RS. Effect of increased expression of cytoskeletal protein vinculin on ischemia-reperfusion injury in ventricular myocytes. *American journal of physiology Heart and circulatory physiology*. 2003; 284:H911–918. [PubMed: 12578817]
26. Haslam G, Wyatt D, Kitos PA. Estimating the number of viable animal cells in multi-well cultures based on their lactate dehydrogenase activities. *Cytotechnology*. 2000; 32:63–75. [PubMed: 19002967]
27. Chen Y, Chen Y, Zhao L, Chen Y, et al. Inflammatory stress exacerbates hepatic cholesterol accumulation via disrupting cellular cholesterol export. *Journal of gastroenterology and hepatology*. 2012; 27:974–984. [PubMed: 22098164]
28. Du F, Yu F, Wang Y, Hui Y, et al. MicroRNA-155 deficiency results in decreased macrophage inflammation and attenuated atherogenesis in apolipoprotein E-deficient mice. *Arterioscler Thromb Vasc Biol*. 2014; 34:759–767. [PubMed: 24504735]
29. Andrae J, Gallini R, Betsholtz C. Role of platelet-derived growth factors in physiology and medicine. *Genes & development*. 2008; 22:1276–1312. [PubMed: 18483217]
30. Singh RB, Mengi SA, Xu YJ, Arneja AS, Dhalla NS. Pathogenesis of atherosclerosis: A multifactorial process. *Experimental and clinical cardiology*. 2002; 7:40–53. [PubMed: 19644578]
31. Perez-Vizcaino F, Cogolludo A, Moreno L. Reactive oxygen species signaling in pulmonary vascular smooth muscle. *Respiratory physiology & neurobiology*. 2010; 174:212–220. [PubMed: 20797450]
32. Greig FH, Kennedy S, Spickett CM. Physiological effects of oxidized phospholipids and their cellular signaling mechanisms in inflammation. *Free radical biology & medicine*. 2012; 52:266–280. [PubMed: 22080084]
33. Zhang C, Zhao YX, Zhang YH, Zhu L, et al. Angiotensin-converting enzyme 2 attenuates atherosclerotic lesions by targeting vascular cells. *Proceedings of the National Academy of Sciences of the United States of America*. 2010; 107:15886–15891. [PubMed: 20798044]
34. Rodriguez A. Novel molecular aspects of ghrelin and leptin in the control of adipobiology and the cardiovascular system. *Obesity facts*. 2014; 7:82–95. [PubMed: 24685565]
35. Haider UG, Roos TU, Kontaridis MI, Neel BG, et al. Resveratrol inhibits angiotensin II- and epidermal growth factor-mediated Akt activation: role of Gab1 and Shp2. *Molecular pharmacology*. 2005; 68:41–48. [PubMed: 15849355]
36. Chaussade C, Rewcastle GW, Kendall JD, Denny WA, et al. Evidence for functional redundancy of class IA PI3K isoforms in insulin signalling. *Biochem J*. 2007; 404:449–458. [PubMed: 17362206]
37. Kunjathoor VV, Febbraio M, Podrez EA, Moore KJ, et al. Scavenger receptors class A-I/II and CD36 are the principal receptors responsible for the uptake of modified low density lipoprotein

- leading to lipid loading in macrophages. *The Journal of biological chemistry*. 2002; 277:49982–49988. [PubMed: 12376530]
38. Iwata H, Aikawa M. Liver-artery interactions via the plasminogen-CD36 axis in macrophage foam cell formation: new evidence for the role of remote organ crosstalk in atherosclerosis. *Circulation*. 2013; 127:1173–1176. [PubMed: 23509031]
 39. Collot-Teixeira S, Martin J, McDermott-Roe C, Poston R, McGregor JL. CD36 and macrophages in atherosclerosis. *Cardiovascular research*. 2007; 75:468–477. [PubMed: 17442283]
 40. Chang YC, Lee TS, Chiang AN. Quercetin enhances ABCA1 expression and cholesterol efflux through a p38-dependent pathway in macrophages. *Journal of lipid research*. 2012; 53:1840–1850. [PubMed: 22711909]
 41. Yin K, Liao DF, Tang CK. ATP-binding membrane cassette transporter A1 (ABCA1): a possible link between inflammation and reverse cholesterol transport. *Molecular medicine*. 2010; 16:438–449. [PubMed: 20485864]
 42. Vallejo JG. Role of toll-like receptors in cardiovascular diseases. *Clinical science*. 2011; 121:1–10. [PubMed: 21413930]
 43. Edfeldt K, Swedenborg J, Hansson GK, Yan ZQ. Expression of toll-like receptors in human atherosclerotic lesions: a possible pathway for plaque activation. *Circulation*. 2002; 105:1158–1161. [PubMed: 11889007]
 44. Geng HL, Lu HQ, Zhang LZ, Zhang H, et al. Increased expression of Toll like receptor 4 on peripheral-blood mononuclear cells in patients with coronary arteriosclerosis disease. *Clinical and experimental immunology*. 2006; 143:269–273. [PubMed: 16412050]
 45. Li H, Sun B. Toll-like receptor 4 in atherosclerosis. *Journal of cellular and molecular medicine*. 2007; 11:88–95. [PubMed: 17367503]
 46. Carpenter KL, Taylor SE, van der Veen C, Williamson BK, et al. Lipids and oxidised lipids in human atherosclerotic lesions at different stages of development. *Biochimica et biophysica acta*. 1995; 1256:141–150. [PubMed: 7766691]
 47. Guo X, Nie L, Esmailzadeh L, Zhang J, et al. Endothelial and smooth muscle-derived neuropilin-like protein regulates platelet-derived growth factor signaling in human vascular smooth muscle cells by modulating receptor ubiquitination. *The Journal of biological chemistry*. 2009; 284:29376–29382. [PubMed: 19696027]
 48. Gerthoffer WT. Mechanisms of vascular smooth muscle cell migration. *Circulation research*. 2007; 100:607–621. [PubMed: 17363707]
 49. Chen Z, Lee FY, Bhalla KN, Wu J. Potent inhibition of platelet-derived growth factor-induced responses in vascular smooth muscle cells by BMS-354825 (dasatinib). *Molecular pharmacology*. 2006; 69:1527–1533. [PubMed: 16436588]
 50. Butoi ED, Gan AM, Manduteanu I, Stan D, et al. Cross talk between smooth muscle cells and monocytes/activated monocytes via CX3CL1/CX3CR1 axis augments expression of pro-atherogenic molecules. *Biochimica et biophysica acta*. 2011; 1813:2026–2035. [PubMed: 21888931]
 51. Jiang P, Xu J, Zheng S, Huang J, et al. 17beta-estradiol down-regulates lipopolysaccharide-induced MCP-1 production and cell migration in vascular smooth muscle cells. *Journal of molecular endocrinology*. 2010; 45:87–97. [PubMed: 20538789]
 52. Sadeghi MM, Glover DK, Lanza GM, Fayad ZA, Johnson LL. Imaging atherosclerosis and vulnerable plaque. *Journal of nuclear medicine : official publication, Society of Nuclear Medicine*. 2010; 51(Suppl 1):51S–65S.
 53. Tan X, Yang L, Xian L, Huang J, et al. ATP-binding cassette transporter A1 (ABCA1) promotes arsenic tolerance in human cells by reducing cellular arsenic accumulation. *Clinical and experimental pharmacology & physiology*. 2014; 41:287–294. [PubMed: 24552478]
 54. Matsumoto K, Hirano K, Nozaki S, Takamoto A, et al. Expression of macrophage (Mphi) scavenger receptor, CD36, in cultured human aortic smooth muscle cells in association with expression of peroxisome proliferator activated receptor-gamma, which regulates gain of Mphi-like phenotype in vitro, and its implication in atherogenesis. *Arteriosclerosis, thrombosis, and vascular biology*. 2000; 20:1027–1032.

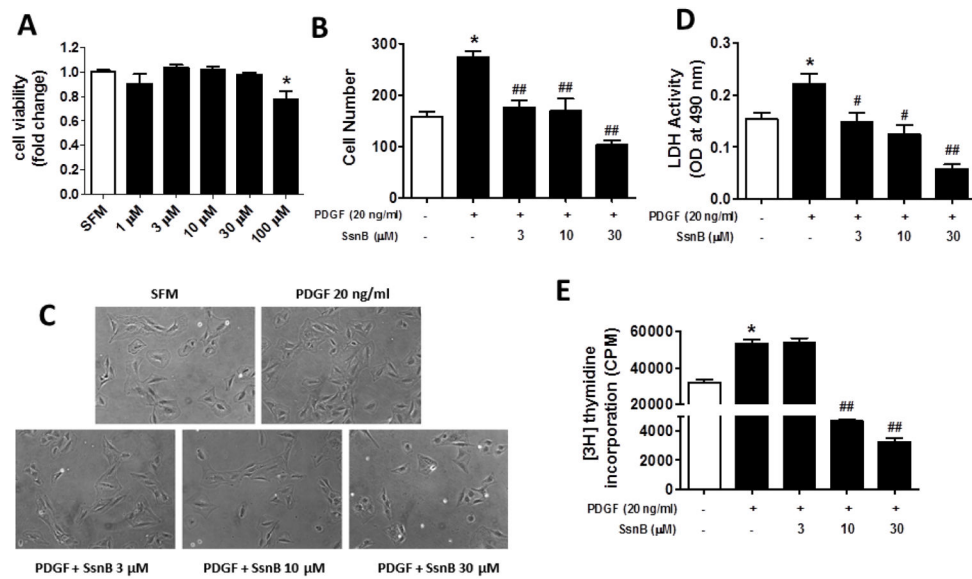


Figure 1. SsnB suppresses PDGF-induced VSMC proliferation

Rat VSMCs were treated with SsnB (0–100 μM) in serum-free medium (SFM) for 24 h, cell viability was determined by LDH assay (A). Rat VSMCs were treated with PDGF (20 ng/ml in SFM) with or without SsnB for 24 h. Cell proliferation was determined by direct cell counting (cell number per 100x field; B) and LDH assay (D). Data are presented as Mean ± SEM, n=3. C. Representative images for results presented in panel B. Magnification: 100x. E. Proliferation of VSMCs was determined by [³H] thymidine incorporation assay. [³H] thymidine at 1 μCi/ml was added to the medium and the cells were then cultured for 24 h. Data are presented as Mean ± SEM, n=6. **p*<0.05 vs SFM group, #*p*<0.05, ##*p*<0.01 vs PDGF group.

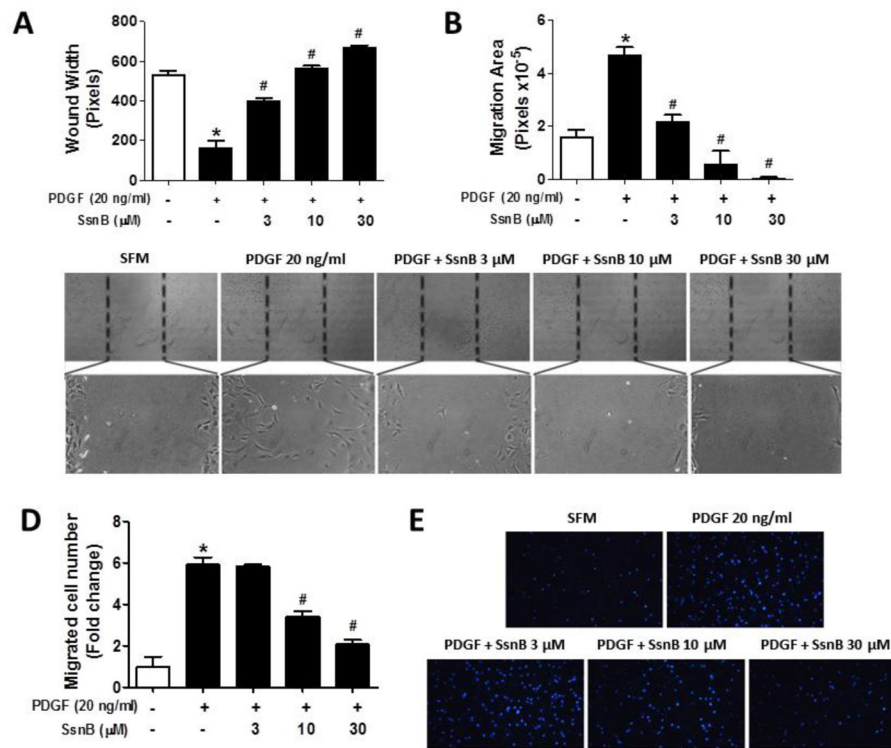


Figure 2. SsnB inhibits PDGF-induced VSMC migration

A–C. Wound healing assays were performed as described in Methods. Five images (Magnification: 100X) in each sample were taken and the wound width (**A**) and migration area (**B**) were analyzed by Image-Pro Plus 6.0 software. Data are presented as Mean \pm SEM, $n=3$. Representative images were obtained from each group (**C**). **D–E.** Transwell migration assays were performed as described in Methods. **D.** Five images in each sample were taken and the migrated cell numbers were analyzed by Image-Pro Plus 6.0 software. Data are presented as Mean \pm SEM of three independent experiments. **E.** Representative images were taken under a wide-field fluorescence microscope (100 \times). * $p<0.05$ vs SFM group, # $p<0.01$ vs PDGF group.

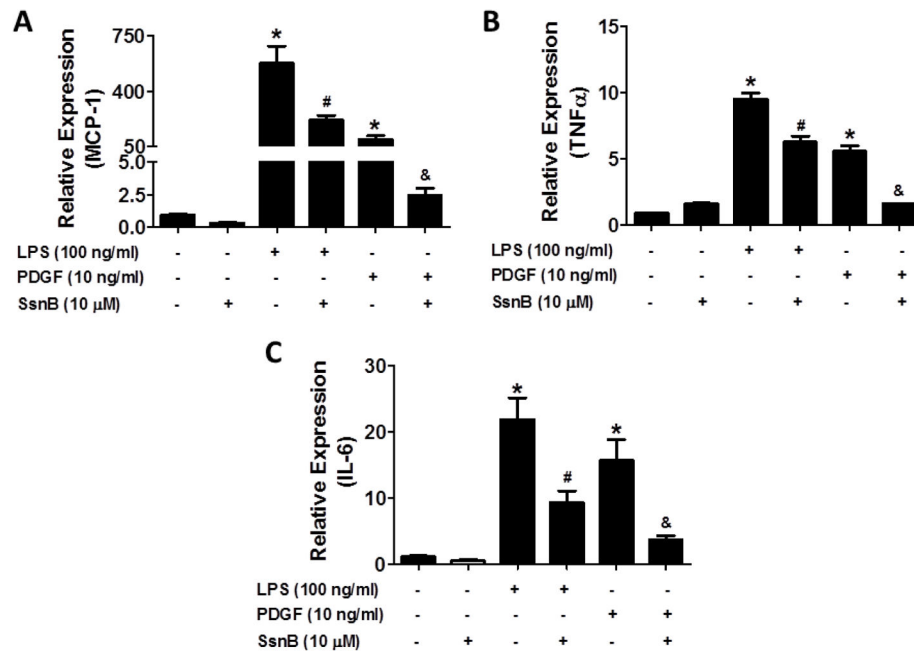


Figure 3. SsnB suppresses LPS or PDGF-induced expression of inflammatory mediators in VSMCs

VSMC were stimulated by LPS (100 ng/ml) or PDGF (20 ng/ml) in the absence or presence of SsnB (10 μM) for 24 h. MCP-1 (A), TNFα (B) and IL-6 (C) mRNA levels (normalized by 18S) were determined by qRT-PCR. Data are presented as Mean ± SEM, n=3. * p <0.05 vs SFM control group, # p <0.05 vs LPS group; & p <0.05 vs PDGF group.

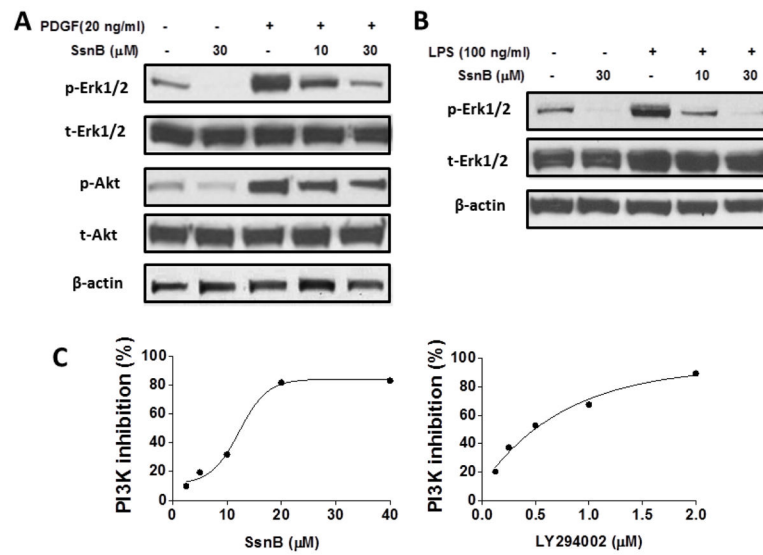


Figure 4. SsnB suppresses Erk and Akt signaling pathways in VSMCs

A. VSMCs were stimulated by PDGF (20 ng/ml) in the absence or presence of SsnB (10 and 30 μ M) for 6 h. Total Erk1/2 and Akt (t-Erk1/2, t-Akt) and phosphorylated Erk1/2 and Akt (p-Erk1/2, p-Akt) protein levels were determined by western Blot. **B.** VSMCs were stimulated by LPS (100 ng/ml) in the absence or presence of SsnB (10 and 30 μ M) for 6 h. t-Erk1/2 and p-Erk1/2 protein levels were determined by western Blot. Representative blots of 3 experiments are shown. **C.** Inhibition of PI3K p100 α kinase activity by SsnB was measured by ELISA as described in methods. LY294402 was used as a positive control.

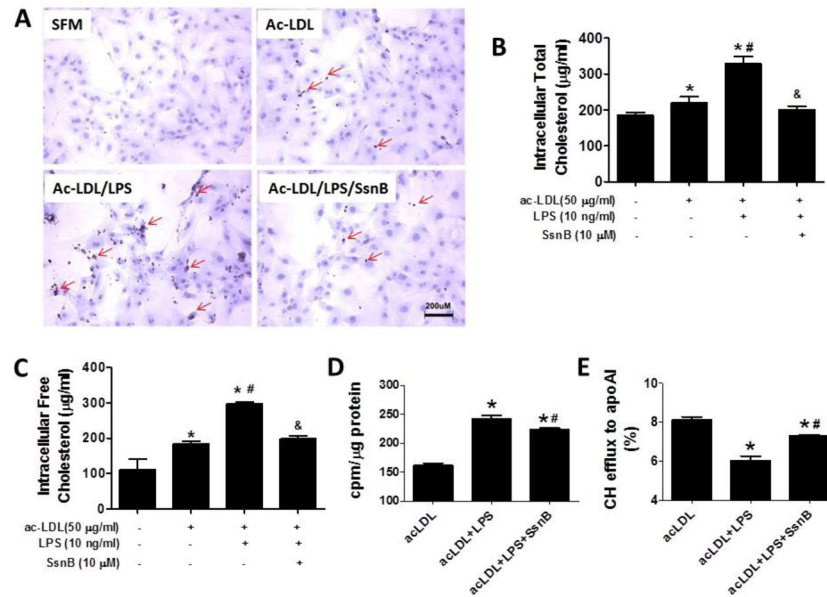


Figure 5. SsnB attenuates cholesterol accumulation in acetylated LDL-loaded VSMCs
A. VSMCs were treated with ac-LDL (50 µg/ml) without SsnB and ac-LDL plus LPS (10 ng/ml) in the absence or presence of SsnB (10 µM) for 24 h. Oil Red O staining was performed to detect the intracellular lipid accumulation. Ten images in each sample were taken under a phase contrast microscope. Lipids appeared dark red and nuclei appeared blue. Representative images are shown. In a different set of experiment, intracellular total cholesterol (**B**) and free Cholesterol (**C**) levels were determined by Intracellular Cholesterol Detection Kit. Data are presented as Mean ± SEM, n=3. * p <0.05 vs untreated group, # p <0.05 vs ac-LDL group, & p <0.05 vs ac-LDL plus LPS group. VSMCs were loaded with ³H-cholesterol incorporated ac-LDL and cholesterol efflux to apoAI was measured. Total cholesterol loading (cpm/µg cellular protein) (**D**) and the efficiency of cholesterol efflux to apoAI (**E**) were shown. Data are presented as Mean ± SEM, n=3. * p <0.05 vs acLDL, # p <0.05 vs acLDL+LPS.

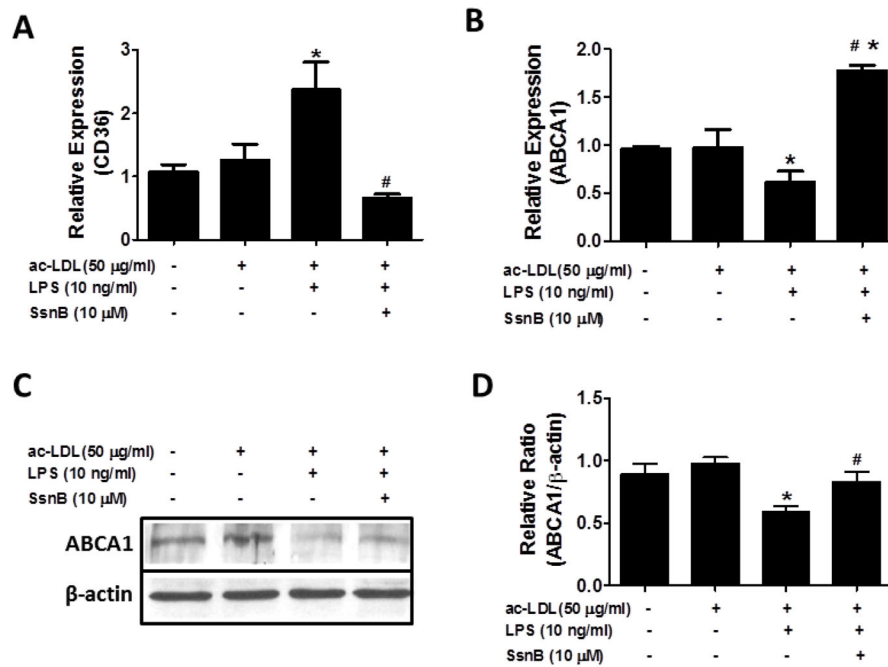


Figure 6. SsnB alters CD36 and ABCA1 expression

VSMCs were treated with ac-LDL (50 μ g/ml) without SsnB and ac-LDL plus LPS (10 ng/ml) in the absence or presence of SsnB (10 μ M) for 24 h. CD36 (A) and ABCA1 (B) mRNA levels were determined by qRT-PCR. ABCA1 protein level was determined by western blot (C and D). Data are presented as Mean \pm SEM. $n=3$, * $p<0.05$ vs untreated group and ac-LDL group, # $p<0.05$ vs ac-LDL plus LPS group.